REVIEW

RJME
Romanian Journal of Morphology & Embryology
http://www.rjme.ro/

Usefulness of ultrastructure studies for the estimation of the postmortem interval. A systematic review

SORIN HOSTIUC[1)], MUGUREL CONSTANTIN RUSU[2,3)], VASILE SORIN MĂNOIU[4)], ALEXANDRA DIANA VRAPCIU[2)], IONUŢ NEGOI[5)], MARIA VIORELA POPESCU[2)]

[1)]*Division of Legal Medicine and Bioethics, Department 2 – Morphological Sciences, Faculty of Medicine, "Carol Davila" University of Medicine and Pharmacy, Bucharest, Romania*

[2)]*Division of Anatomy, Department 1, Faculty of Dental Medicine, "Carol Davila" University of Medicine and Pharmacy, Bucharest, Romania*

[3)]*MEDCENTER, Center of Excellence in Laboratory Medicine and Pathology, Bucharest, Romania*

[4)]*Department of Cellular and Molecular Biology, National Institute of Research and Development for Biological Sciences, Bucharest, Romania*

[5)]*Department of Surgery, Faculty of Medicine, "Carol Davila" University of Medicine and Pharmacy, Bucharest, Romania*

Abstract

Establishing the postmortem interval (PMI) is vital in legal medicine as it allows to retrospectively estimate the hour of death, which is essential for the police as a starting point for their inquiries (especially in violent deaths). Ultrastructure studies aimed specifically to detect autolytic changes are scarcely identified in the scientific literature. Moreover, they are performed in a variety of conditions (different temperatures, species, *in vitro* / *in situ*, and so on), making the results difficult to interpret for legal medicine purposes. The main aim of this review is to determine the potential usefulness of ultrastructure studies for the estimation of the postmortem interval and to provide a summary of relevant scientific literature in the area, which might be useful as a starting point for more specific and detailed studies in the field. We performed a search on the *ISI Thomson Web of Knowledge* database using a series of predefined keywords; the articles fulfilling the inclusion criteria were systematically analyzed to identify ultrastructure changes associated with autolysis. Our investigation revealed 20 relevant articles, which detailed ultrastructure changes in the brain, heart, liver, pancreas, kidney, bone, sweat glands, thyroid, skeletal muscle, cartilage and sweat glands. For each organ, we arranged systematically postmortem ultrastructure changes that were described by various authors. Ultrastructure changes appear early and may be useful in determining the time since death in the early postmortem interval. However, most studies published in this area followed methodologies that could not allow a proper reproducibility in forensic circumstances. Therefore, before using ultrastructure for estimating the PMI in practical environments, further studies are needed. They should be performed ideally on human samples, obtained at regular intervals after death, at variable, decreasing temperatures.

Keywords: ultrastructure, autolysis, estimating the postmortem interval, postmortem interval in forensic practice.

Introduction

Establishing the postmortem interval (PMI) is paramount in legal medicine as it allows to retrospectively estimate the moment of death, which is essential for the police as a starting point for their inquiries (especially in violent deaths). There are five main methods of establishing the PMI, routinely used in forensic practice: purely physical processes (lividity, *algor mortis*), physicochemical processes (*rigor mortis*), metabolic processes (supravital reactions), autolysis, and putrefaction [1].

Death, from a medical point of view, is defined as the irreversible cessation of respiratory, circulatory and cerebral functions. Biologically, death is a process for which are defined, mostly for practical reasons a series of predefined steps. With the irreversible cessation of the circulatory function, the organs, tissues and cells enter in a process called supravital period or intermediate life. The absence of the blood flow leads locally to a rapid consumption of the oxygen and subsequently to a shift toward the anaerobic metabolism. Gradually, all locally available nutrients are catabolized through anaerobic mechanisms, the energy-dependent cellular mechanisms cease to function, causing irreversible changes to the organic structures [2, 3]. They are known under the general term autolysis and chiefly include abacterial destruction of tissues by hydrolytic, lysosomal enzymes [4], but also other processes like hydro-electrolyte disturbances caused by the function cease of the ionic pumps [5].

The speed of autolytic processes is influenced by temperature (direct correlation), humidity, preexistent pathologies (sepsis, hyperthermia increases the rate, while hypothermia decreases it), and especially the histological characteristics of individual organs. The speed is higher in organs with a large concentration of lytic enzymes (pancreas), increased water content (pancreas, spleen), a decreased conjunctive matrix (heart, brain, lungs, endothelia), or that are bathed in corrosive liquids (stomach) [6]. Autolytic processes can be identified during the gross examination of the body or by using various histological, biochemical or ultrastructure methods [7–14]. Currently, the most often used techniques for establishing the postmortem interval are temperature, postmortem muscle excitability and the variation of different chemical or biochemical substances in various fluids (mainly vitreous humor, but also blood, pericardial fluid, and so on)

[3, 5]. Each method is prone to errors, and forensic pathologists try to minimize them by combining two or more approaches for each case. Sometimes, however, obtaining relevant data from two or more techniques can be extremely difficult, or even impossible. Therefore, each new, potentially useful method in establishing the postmortem interval may be beneficial in specific cases/ circumstances.

Ultrastructure studies aimed specifically to detect autolytic changes are scarcely identified in the scientific literature. Moreover, they are performed in a variety of conditions (different temperatures, species, *in vitro* / *in situ*, and so on), making the results difficult to interpret in a forensic context. However, many of the established precise intervals for the appearance of various ultrastructure changes after death [11, 15, 16]. Therefore, we hypothesized that, if environment factors could be properly controlled, ultrastructure studies might be extremely useful in establishing the postmortem interval in humans.

The purpose of this review is to analyze the potential usefulness of ultrastructure studies to the estimation of the postmortem interval and to provide a summary of relevant scientific literature in the area, which could be useful as a starting point for more specific and detailed studies in the field.

Methodology of review

We performed a search on the *ISI Thomson Web of Knowledge* database using the following keywords: ultrastructure + postmortem, which yielded 139 results (time range 1970–2016), electron microscopy + postmortem, which yielded 543 results, and autolysis + electron microscopy, which yielded 57 results. We excluded articles without an abstract those found in print editions only [17], those analyzing ultrastructure changes associated with various pathologies (*e.g.*, [18]), even if they showed time-dependent postmortem ultrastructure changes (except those who had a control group, cases which we detailed in this article). For each relevant article, we also performed an analysis of the list of references.

Relevant publications

Our analysis identified 21 relevant articles, which analyzed ultrastructure changes in the brain, heart, liver, pancreas, kidney, bone, sweat glands, thyroid, skeletal muscle, cartilage and sweat glands. Details are found in Table 1.

Table 1 – ***The main studies included in the analysis***

Structure	Species	Temperature	Postmortem intervals	Reference
Brain	Rat	Environment	1, 3, 6, 9, 12, 24 hours	[19]
Brain	Cat	Body temperature	30, 90 minutes	[20]
Heart	Rat	4^0C	0, 1, 2, 4, 8, 24, 28, 32, 48 hours	[7]
Heart	Rat	19^0C	10, 30 minutes, 1, 4, 12 hours, 1, 2, 4, 8, 12, 16, 20 days	[15]
Heart	Rat	20^0C	15 minutes, 1, 3, 5, 10 hours	[21]
Heart	Dog	22^0C	15, 45, 120, 240 minutes	[22]
Heart	Rat	23^0C	1, 3, 5, 10, 15, 24 hours	[11]
Heart	Rat	Environment	0, 2, 4 hours	[23]
Heart	Dog	37^0C	15, 30, 60, 120, 180 minutes	[24]
Heart	Human	Room temperature for the first two hours; afterwards, at 4^0C	20, 60, 90, 120 minutes, 3, 6, 12, 15, 18 hours	[25]
Liver	Rat	8, 18, 28^0C	0, 2, 4, 6, 12, 24 hours	[16]
Liver	Human	18^0C	6, 12, 24 hours	[16]
Liver	Rat	23^0C	1, 3, 5, 10, 15, 24 hours	[11]
Liver	Rat	Environment	0, 2, 4 hours	[23]
Liver	Rat	Body temperature	15, 30, 60, 120 minutes	[26]
Pancreas	Rat	23^0C	1, 3, 5, 10, 15, 24 hours	[11]
Pancreas	Rat	Environment	0, 2, 4 hours	[23]
Pancreas	Rat	37^0C	0, 0.5, 1, 2, 4, 8, 16 hours	[27]
Kidney	Rat	0^0C (20, 48, 72 hours) Environment: 20^0C, 48^0C	20, 48, 72 hours	[28]
Kidney	Rat	22 ± 3^0C	0, 1, 5, 10, 15, 20 hours	[29]
Kidney	Rat	Environment	4, 9, 12, 24, 48 hours	[9]
Kidney	Rat	23^0C	1, 3, 5, 10, 15, 24 hours	[11]
Skeletal muscle	Rat	23^0C	1, 3, 5, 10, 15, 24 hours	[11]
Skeletal muscle	Mouse	Environment ($10–20^0$C)	5–10 minutes, 3, 6, 12, 24, 48 hours	[8]
Thyroid	Rat	Unspecified	0, 60 minutes	[30]
Intervertebral disk	Mouse	4^0C	0, 1, 6, 12, 24 hours	[31]
Bones	Human	Environment	Up to 15 years	[10]
Sweat glands	Human	Environment	3, 6, 9, 12 hours	[32]

Cerebral autolytic changes

There is a scarcity of articles dealing with ultrastructure changes caused by autolysis in the brain. Arsénio-Nunes *et al.* (1973) analyzed the ultrastructure changes in the cat brain, 30 and 90 minutes after the arrest of the cerebral circulation [20]. Sheleg *et al.* (2008) analyzed the ultra-structure of rat brain at 0, 3, 6, 9, and 12 hours after death [19]. The earliest postmortem changes, found at 30 minutes, were represented by an enlargement of the glial and neuronal processes in the molecular layer. In other layers of the brain, the neuropil was sometimes swollen, but the change was less significant compared to the molecular layer. Astrocytes presented swellings mostly

in the vascular end feet and scarcer in the perikarya [20]. Neurons presented only a slight volume increase of the endoplasmic reticulum. The endothelial cells of the capillary walls had a high number of pinocytotic vesicles and marginal folds and flaps, which were projecting toward the lumen [20]. At 90 minutes of ischemia, the molecular and external granular layers were severely swollen. Mitochondrial damage was frequent, with swelling and breakage of mitochondrial cristae. The other layers presented astrocyte perikaryal and perivascular swelling. Neurons were well preserved, the only obvious change being a swelling of the endoplasmic reticulum. Endothelial cells had a lower density of pinocytic vesicles compared to the changes encountered at 30 minutes [20]. At three hours, the neuronal mitochondria were sometimes swollen [19]. After six hours, the authors encountered vacuolizations of the endoplasmic reticulum and lysosomes associated with clumping of the neuronal chromatin. At nine hours, the ribosomes tended to disappear from neurons, while at 24 hours was identifiable a complete chromatolysis in 72% of the cortical neurons [19].

Cardiac autolysis in transmission electron microscopy (TEM)

Autolysis in the heart was intensely studied, mostly in rats [4, 21] and dogs [22, 24], on variable temperatures, from 4^0C [7] to 37^0C [24], from very early changes [22] to those occurring 20 days after death [15]. Details regarding the postmortem changes are presented in Table 2 and Figures 1 and 2.

Table 2 – ***Ultrastructure changes in the heart, depending on the postmortem interval***

Postmortem interval	Ultrastructural changes
< 30 minutes	Nucleus: chromatin margination [15, 24]; slight clumping [21] Mitochondria: moderate enlargement [15]; decreased matrix density [24]; occasional fragmentation of the outer membrane [24, 25]; few amorphous matrix densities [25] Endoplasmic reticulum: enlargement and enrounding [15] Lysosomes: present [15] Myofibrils: I band not clearly discernable from H band [21] Glycogen: some loss of glycogen [15] / decreased glycogen [21, 24]
1 hour	Nucleus: chromatin clumping [11, 21]; chromatin margination [24] Mitochondria: inconstant broken cristae [7]; mitochondria number decreased to about a half but density increased by a third [22]; mean outer surface doubled [22]; increased mitochondrial volume [24, 25] (doubled [23]); dense granules [24, 25] Endoplasmic reticulum: inconstant dilation of transverse tubules [7]; occasional vacuolation [24] Myofibrils: relaxed [7]; enlarged interfibrillar spaces [24]; prominent I, H bands [7]; thickening of / around the I band, clearly discernable from H band; no distinct I band [24]; poorly defined H band [24] Glycogen: still abundant [7]; very rare [21, 24]
2 hours	Mitochondria: swelling, broken cristae [7]; amorphous densities [22], more often and bigger compared to one hour [24]; volume increased by 25% compared to one hour [23] Lysosomes: present [15] Myofibrils: inconstantly contracted [7] Glycogen: present [4]; small quantities [15]
3 hours	Mitochondria: swelling [11]; advanced fragmentation and vesiculation [25] Myofibrils: obvious I bands [11] Glycogen: absent [11] Cytoplasm & cell membrane: slight cell edema [11]
4 hours	Mitochondria: swollen, most with broken cristae; pleomorphic; dense bands of apparently fused cristae [7] Endoplasmic reticulum: extremely swollen, irregular surface [22] Lysosomes: present [15] Myofibrils: large spaces between myofibrils, causing vacuoles [22]; obvious I lines [22]
8 hours	Nucleus: chromatin clumping [7] Mitochondria: swollen, with large vacuoles, dense bands of fused cristae [4] Myofibrils: pushed laterally by swollen mitochondria (initial indication of fiber disruption) [7] Glycogen: reduced quantities [7]
10 hours	Endoplasmic reticulum: dilated [11] Lysosomes: absent [15]
12 hours	Glycogen: absent [15]
15–16 hours	Mitochondria: amorphous, dense deposits [11] Cytoplasm: moderate cell edema [11]
24 hours	Nucleus: marked chromatin clumping [11] Mitochondria: amorphous, dense deposits [11] Myofibrils: obvious myofibril distortion, loss of parallel arrangement, fragmentation [7]; disorganization of the Z band, separation of the intercalated disk from the opposing membranes [7], I bands present [11] Glycogen: present, reduced quantities [7]
28 hours	Mitochondria: vesiculation and vacuolation [7] Myofibrils: interfibrillar side spaces [7] Glycogen: still present [7]
32 hours	Myofibrils: fractures, fragmentation [7]; poorly organized Z bands, separation of the myofibrils from the Z band [7]
48 hours	Myofibrils: separation and fragmentation [7] Glycogen: greatly reduced but still present [7]
4 days	Nucleus: without chromatin, ghost-like [15] Mitochondria: swollen, some degree of disintegration [15] Myofibrils: no regular and identifiable arrangements [15]
8–12 days	Some myofibers are still identifiable [15] Loss of cell integrity, invasion of bacteria [15]
16–20 days	Rare nuclear ghosts [15] Mitochondria: remained structurally defined, sometimes even with cristae [15] Cells are totally rotten and disintegrated [15]

Liver autolysis in TEM

The autolysis of the liver was studied primarily on rats, and mainly in warmer environments (either room temperature [23] or body temperature [26]). Details regarding the postmortem changes are presented in Table 3.

Table 3 – ***Ultrastructure changes in the liver, depending on the postmortem interval***

Postmortem interval	Ultrastructural changes
< 30 minutes	Mitochondria: swollen (at 30 minutes, but not at 15 minutes) [26] Endoplasmic reticulum: fragmentation (inconstant at 15 minutes, increased at 30 minutes), beadlike enlargements [26]; inconstant detachment of ribosomes at 30 minutes [26] Glycogen: depends on the fed / fasted status [26]

Postmortem interval	Ultrastructural changes
< 30 minutes	Cell membrane: disappearance of microvilli along the sinusoidal border adjacent to the space of Disse [26]; expansion and focal interruption of the plasma membrane [26]
1 hour	Nucleus: chromatin clumping [11] Mitochondria: severely swollen, loss of mitochondrial cristae [26] Endoplasmic reticulum: swollen [26] Golgi apparatus: dilatation of sacs and vesicles [26] Lysosomes: increased number, enlarged, sometimes lack the dense opaque core [26]
2 hours	Nucleus: crenation and vacuolar detaching of nuclear membranes, granulation and clumping of chromatin (28^0C, rat) [16] Mitochondria: severely swollen [26], around 12% increase in volume [23]; disappearance of cristae, interruption of the mitochondrial membrane, vacuoles [23] Endoplasmic reticulum: more pronounced compared to one hour [26]; marked swelling (28^0C, rat) [16] Golgi apparatus: increased dilatation of sacs and vesicles [26]; marked swelling (28^0C, rat) [16] Cytoplasm and cell membrane: pallor, enlargement, interdigitating membranes lining bile canaliculi [23]; microvilli lining the sinusoidal border are absent [23]
4 hours	Nucleus: swelling and slight granularity of the chromatin [16]; partial lysis of the outer nuclear membrane (28^0C, rat) [16] Mitochondria: no significant volume increase compared to two hours [23] Cytoplasm: vacuolization (28^0C, rat) [16]
6 hours	Nucleus: peripheral migration of chromatin, partial lysis of the outer nuclear membrane (18^0C) [16]; lysis of the inner nuclear membrane with leakage of chromatin (28^0C, rat) [16] Mitochondria: initial homogenization of the mitochondrial matrix (8^0C) [16] Significant loss of mitochondrial cristae (28^0C, rat) [16] Endoplasmic reticulum: initial lysis (18^0C) [16] Golgi apparatus: swelling and turbidness (18^0C) [16] Glycogen: decreased (28^0C, rat) [16] Cytoplasm: vacuolization (18^0C) [16]
10 hours	Mitochondria: amorphous, dense bodies, inconstant [11]
12 hours	Nucleus: separation of the nuclear membranes (8^0C, rat) [16]; initial lysis of the inner membrane, occasional leakage of chromatin in the cytoplasm (18^0C) [16] Mitochondria: amorphous deposits in the mitochondrial matrix (18^0C, 28^0C) [16] Endoplasmic reticulum: complete lysis (28^0C, rat) [16] Golgi apparatus: complete lysis (28^0C, rat) [16] Cytoplasm: vacuolization (18^0C, 28^0C) [16]
15 hours	Mitochondria: significant amorphous dense bodies [11]
24 hours	Nucleus: diffuse leakage of chromatin in the cytoplasm (18^0C) [16] Mitochondria: shape deformation, numerous amorphous bodies (18^0C) [16]; lysis of the outer mitochondrial membrane (28^0C, rat) [16] Endoplasmic reticulum: diffuse, moderate lysis (18^0C) [16] Golgi apparatus: diffuse, moderate lysis (18^0C) [16] Glycogen: initial reduction of glycogen granules (8^0C, 18^0C rat) [16]; marked reduction (28^0C, rat) [16]

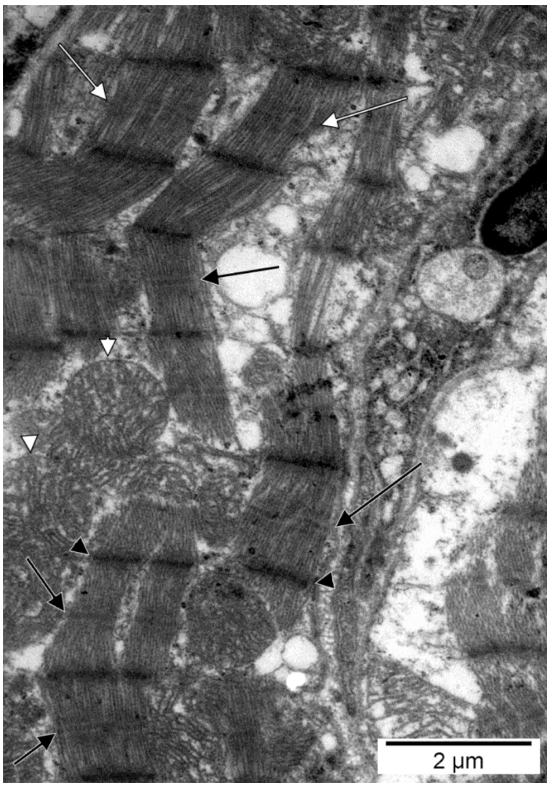

Figure 1 – ***Rat myocardium. TEM of a one-hour post-mortem interval ventricular sample, prepared as described in [23]. Enlarged interfibrillary spaces. Heterogeneity of the myofibrillar bands: I bands clearly discernable (black arrows) from H bands (black arrowheads), as well as I bands not clearly discernable (white arrows). Enlarged mitochondria (white arrowheads) seemingly lack an outer membrane. (Photo from the personal collection of the authors).***

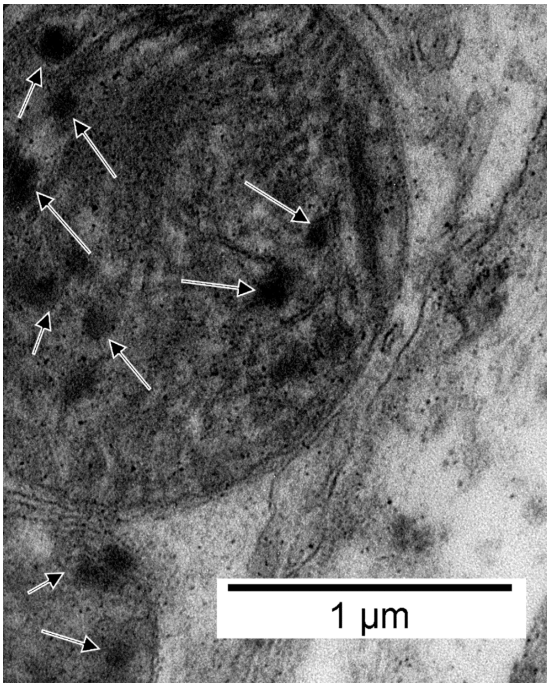

Figure 2 – ***Rat myocardium. TEM of a two-hour post-mortem interval ventricular sample, prepared as described in [23]. Mitochondrial amorphous dense deposits, rather than dense granules, are indicated (arrows). The increased mitochondrial volume is evident. (Photo from the personal collection of the authors).***

Pancreas autolysis in TEM

The autolysis of the pancreas was studied mostly on rats, and mainly in warmer environments (either room temperature [23] or body temperature [27]). Compared to other organs, the changes tended to appear more rapidly, and the speed of changes was increased. See Table 4 for details and Figure 3 for an example.

Table 4 – ***Ultrastructure changes in the pancreas, depending on the postmortem interval***

Postmortem interval	Ultrastructural changes
30 minutes	Mitochondria: swollen, round or oval [11]
1 hour	Nucleus: chromatin clumping [23, 27] Mitochondria: amorphous dense bodies [11] Endoplasmic reticulum: slight dilatation [11, 27] Secretory granules: fused with the apical membrane [27]
2 hours	Nucleus: chromatin condensation [23] Mitochondria: volume more than doubled compared to 0 h postmortem; disappearance of cristae, interruptions of the membrane, vacuoles, spiralous membranous profiles [23]; paler matrix, some myelin figures in the matrix [27] Endoplasmic reticulum: dilatation, fragmentation and vesiculation; vacuoles with concentrically arranged membranes [23] Secretory granules: increased size (condensation of granules) [27] Cytoplasm and cell membrane: pallor, interdigitations, and enlargement of the membranes lining the acinar lumen [23]; interruptions / blebs on the lateral side of the membranes [23]; separation of desmosomes and intermediate junctions [23]
4 hours	Mitochondria: volume tripled compared to 0 h postmortem [23]; large, electron dense particles [23] Endoplasmic reticulum: increased vesiculation and fragmentation [23]
8 hours	Nucleus: loss of the nuclear envelope [23] Mitochondria: hard to identify after eight hours [27] Endoplasmic reticulum: disintegration or arrangement in fingerprint-like concentric whorls [27]; irregular, fluffy densities along the cisterns [27] Secretory granules: still identifiable [27] Cell membrane: almost complete conversion of the membrane into myelin figures [27]
15–16 hours	Nucleus: karyolysis [23] Mitochondria: marked degeneration [11] Endoplasmic reticulum: poorly defined cisternae [23] Secretory granules: inconstant deposits of crystalline materials [27]
24 hours	Disappearance of organelles, cell shrinkage [11]

Kidney autolysis in TEM

The autolysis of the kidney was studied mostly on rats, either at 0^0C or around 20^0C [9, 11, 28, 29]. The speed of autolytic changes seems lower compared to other organs (especially the pancreas), but it is very different depending on the location (more intense in the distal tubules compared to the proximal tubules). More details in Table 5.

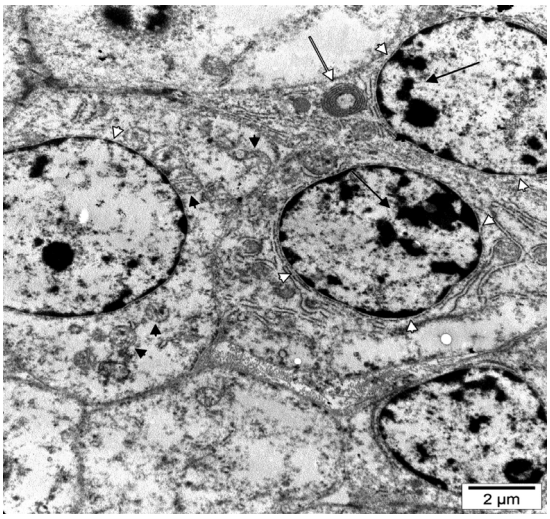

Figure 3 – ***Human fetal pancreas. TEM of an eight-hour postmortem sample, prepared as described in [23]. Chromatin condensation (black arrows), cytoplasmic whorls (white arrow), interrupted nuclear envelopes (white arrowheads) and swollen mitochondria (black arrowheads) are indicated. (Photo from the personal collection of the authors).***

Table 5 – ***Ultrastructure changes in the kidney, depending on the postmortem interval***

Postmortem interval	Ultrastructural changes
3 hours	Nucleus: slight clumping of the nuclear chromatin (DT) [11] Mitochondria: slightly swollen (PT) [11] Cell membrane: irregularly arranged microvilli (PT) [11]
4–5 hours	Nucleus: karyopyknosis (more intense in the DT compared to the PT) (22±3^{0}C) [21]; moderate clumping and margination of chromatin (PT) [9, 11]; marked peripheral chromatin condensation, with an inner lucent area containing 1–2 irregular clumps of dense chromatin, crenated nuclear envelope (PT) [9, 11] Mitochondria: swollen (PT) [9, 11]; extensively swelling, vesiculation of cristae (DT) [9] Lysosomes: swollen, with decreased electron density (PT) [9] Cytoplasm and cell membrane: vacuolization (22±3^{0}C, DT, LH) [21]; collapse of the lateral membrane (PT) [9]; collapse of the lateral and apical membrane (DT) [9]
10–12 hours	Nucleus: irregular dilatations of the intermembranous space, blebs, marginal condensation (PT) [9]; uniform, electron dense bodies with slightly irregular outlines and partial or total loss of the nuclear envelope (DT) [9]; marked clumping of chromatin (PT) [11] Mitochondria: interruption of the outer membrane (DT) [9]; amorphous dense bodies (DT) [11] Cytoplasm and cell membrane: lighter, myelin figures close to the brush border, either free of within lysosomes (PT) [9]; myelin figures, lighter (DT) [9]; small vacuoles (PT) [11]; dilatation of the microvilli (PT) [11]
20–24 hours	Nucleus: clumping of the nuclear chromatin (20^{0}C, DT, LH, PT, 0^{0}C – PT) [28] (PT) [11]; complete loss of nuclear envelope, fragmentation of the nuclear bodies (DT) [9] Mitochondria: disruption of the cristae, severe edema (20^{0}C, DT, LH) [29]; amorphous dense bodies (PT) [11] Cytoplasm and cell membrane: vacuolization (20^{0}C, DT, LH) [11]; lamination or rupture of the folding membranes (20^{0}C, DT, LH) [11]

Postmortem interval	Ultrastructural changes
48 hours	Nucleus: markedly shrunk or fragmented, partial or complete lysis of the nuclear membrane [9]; electron dense nuclear bodies; complete loss of nuclear envelope, fragmentation of the nuclear bodies (DT) [9] Cytoplasm and cell membrane: obvious cytolysis (more marked at 20 than at 0^0C, PT – especially in the convoluted tubules); organelles difficult to identify, mostly transformed in cysts full of debris or granules (PT) [9]
72 hours	Nucleus: chromatin margination (0^0C, DT, LH) [28] Mitochondria: swelling (0^0C, DT, LH) [28]

DT: Distal tubule; PT: Proximal tubule; LH: Loop of Henle.

Autolysis in other organs and tissues

Skeletal muscle

Skeletal muscle was intensely studied ultrastructurally, especially for detecting changes associated with *rigor mortis* [8] or for the food industry [33–35]. Tomita *et al.* (2004) studied ultrastructural changes associated with post-mortem autolysis in the skeletal muscle, detecting as landmark shifts in the early postmortem interval the following: contraction at one hour, the appearance of I bands at three hours, and margination of the nuclear chromatin and dense amorphous bodies in some mitochondria at 24 hours [11].

Bone

Yoshino *et al.* (1991) studied the usefulness of estimating the time of death using ultrastructural changes of the skeletal bones. The study dealt with buried / unburied remains; the timeframe was very long (years), and the described changes are mostly putrefactive [10].

Thyroid

McQuade & Evans (1959) studied the autolytic changes in the thyroid one hour after death, finding the following: RE swelling and inconstant fragmentation, mitochondria swelling and vacuolations, and the disappearance of the villi [30].

Intervertebral disk

Higuchi & Abe (1987) studied the ultrastructure changes in the mouse intervertebral disk. In the *annulus fibrosus*, one hour after death was identifiable a slight condensation in the outer region of the nuclei of fibroblast-like cells, a change that was significantly more severe at six hours. Chondrocytes showed not changes at one hour, decreased glycogen content at six hours, karyopyknosis and condensation of the cytoplasm at 12 hours, and severe chondrocyte necrosis at 48 hours. In the cartilage plates, the first changes were identified at six hours – chromatin condensation; at 12 hours, the particles of glycogen decreased in number and chromatin clumping appeared. In the *nucleus pulposus*, the first significant signs appeared at 12 hours when notochordal cells showed abnormal condensation of glycogen particles [31].

Sweat glands

Cingolani *et al.* (1994) studied the usefulness of ultrastructure changes in the sweat glands for estimating the postmortem interval [32]. At three hours, they noticed: a strong reduction in intracellular glycogen (both in clear cells – CC and dark cells – DC), some mitochondrial dilatation (CC, DC, duct cells – dc), lipofuscin granules (CC, DC), initial ER dilatation (CC), and reduction of secretory granules (DC). At six hours, were obvious mitochondrial dilatation with rarefaction of the cristae (CC, DC, dc), an increase in lipofuscin granules (CC) or their initial appearance (DC), ER dilatation, and morphological degeneration of organelles in the outer parts of the myoepithelial cells [32]. At nine hours, the morphological differentiation of the mitochondrial cristae was difficult (CC, DC), the lipofuscin particles increased in number (CC), the secretory capillary and luminal microvilli were rarefied (CC), the luminal cell membrane was rarefied (DC). At 12 hours, the authors found a disappearance of the mitochondrial cristae (CC, DC), karyopyknosis associated with dilatation of the nucleus and the rupture of the nuclear membrane (CC), the disappearance of the capillary microvilli (CC), maximal ER dilatation with immature secretory granules within it (DC). There were also found myoepithelial changes (cytoplasmic vacuolizations, myofilament condensations, nuclear alteration), and changes in the cell membrane of the dc (reduction of cell membrane interdigitations, dilatation of microvilli) [32].

Discussion

Knowing about autolytic, ultrastructure changes has three critical practical consequences: (*1*) it can potentially be used for the estimation of the postmortem interval, (*2*) it allows the differentiation between autolysis- and pathology-related changes identified during the electron microscopy examination [21], an aspect that caused significant methodological issues while performing ultrastructure studies by the authors of this review [14, 36, 37–43], and (*3*) is useful in transplantation from dead donors [16].

By analyzing the results synthesized in Tables 2–5, there are some easily noticeable remarks to be made. Firstly, the changes seem to be highly dependent on the temperature – a lower temperature is associated with a slower autolytic degradation of the samples. This assumption is evident by analyzing the results of Karadžić *et al.* (2010) on liver – for example, at 12 hours and 8^0C is identifiable the separation of the nuclear membranes, while at 28^0C the outer nuclear membrane is partially lysed after only four hours [16]. Ito *et al.* (1991*a*), by studying ultrastructure changes in the kidney, found only a slight swelling of the mitochondria at 0^0C in the distal tubule and the loop of Henle after 24 hours [28], while at environment temperature these structures already presented high amplitude swelling and vesiculation of the cristae at 4–5 hours [9]. In practice, the human body tends to equalize the body temperature with the environment temperature, a process that respects the following equation:

$$Q = \frac{Tr - Ta}{To - Ta} = Ae^{Bt} + (1 - A)e^{\frac{AB}{A-1}t}$$

where Q – standardized temperature; Tr – rectal temperature; Ta – ambient temperature; To – rectal

temperature at death; A, B – constants; t – postmortem interval. B has a value of $-1.2815(m^{-0.625}) + 0.0284$, where m – body weight [47], and A has a value of 1.1 for environment temperatures above 23^0C, and 1.25 for environment temperature below 23^0C [44].

Normally, the environment is colder than the body temperature, and therefore the body temperature decreases after death, in average with 0.8^0C/h [45]. Therefore, if we were to take the environment temperature, as a mean, to be 22^0C, in the first 18–24 hours, after death the body temperature is above this average. Therefore, the autolytic changes should respect the progression obtained at higher temperatures. Most authors however, analyzed the autolytic changes at around 22^0C, a value at which the changes most likely occur slower than in practical instances. Therefore, theoretical models, based on lower temperatures, can only be used in practice for estimating the progression of ultrastructure changes, and not for the actual postmortem interval. The body surface cools faster compared to the internal organs. Cingolani *et al.* (1994) used eccrine glands, with which they established a series of time dependent, morphological changes (histology, ultrastructure, immunohistochemistry) [32]. This approach has, as the main disadvantage, increased dependence on environment factors (environment temperature, humidity, the wind, and so on) [27].

If the temperature is kept constant, the ultrastructure changes seem to have a small time-dependent variation in different studies, a conclusion that is evident in Table 5. Therefore, a proper detection of the ultrastructure changes, at temperatures closer to the ones encountered during the cooling phase of the cadaver, might be useful to estimate the postmortem interval. Further studies in this area are needed, with samples taken at regular interval after death, and with a very detailed (preferably morphometric) analysis of the changes.

The speed of ultrastructure changes differs significantly depending on the organ, with the pancreas being by far the most sensitive, an phenomenon that was proven before [6, 11]. Therefore, if the estimated postmortem interval is low, the pancreas might be the best organ to be from an ultrastructure point of view (if the results at higher temperatures will be proven to be reproducible). If the estimated postmortem interval is higher, other organs might bring more data compared to the pancreas (their ultrastructure changes might still be obvious even if pancreas autolysis is very advanced).

Ultrastructure changes seem to be species-dependent; Karadžić *et al.* (2010) found that human hepatocytes show slower degradation compared to rat hepatocytes when kept at the same temperature [16]. This result should be further analyzed to see whether it is caused by methodological, environment or biological factors.

Limits of the study

A low number of studies that were actually useful in properly establishing the postmortem interval. Some studies seem to have reproducibility issues, which mandate the development of new research in the field, with proper, reproducible methods, directly applied to the establishment of the postmortem interval. We did not analyze potential uses of ultrastructure in pathology, anesthesia, transplantation, as by doing so the study would lose its focus. For example, in transplantation, autolysis could be analyzed in corroboration with the brain dead interval and not only actual postmortem interval.

Conclusions

Ultrastructure changes appear early and may be useful in determining the time since death in the early postmortem interval. However, most studies published in this area followed methodologies that cannot allow a proper reproducibility in forensic circumstances. Therefore, before using ultrastructure for estimating the PMI further studies are needed, ideally on human samples, obtained at regular intervals after death, at variable, decreasing temperatures.

Conflict of interests

The authors declare that they have no conflict of interests.

Author contribution

Authors #1 (SH) and #5 (IN) have equal contributions to this paper.

References

[1] Madea B. Is there recent progress in the estimation of the postmortem interval by means of thanatochemistry? Forensic Sci Int, 2005, 151(2–3):139–149.

[2] Isselhard W. Akuter sauerstoffmangel und wiederbelebung [Acute hypoxia and resuscitation]. Dtsch Med Wschr, 1965, 90(8):349–356.

[3] Madea B. Importance of supravitality in forensic medicine. Forensic Sci Int, 1994, 69(3):221–241.

[4] Haglund WD, Sorg MH (eds). Forensic taphonomy: the postmortem fate of human remains. CRC Press, Boca Raton, FL, USA, 1997.

[5] Dettmeyer R, Verhoff MA, Schütz HF. Forensic medicine: fundamentals and perspectives. Springer-Verlag, Berlin–Heidelberg, 2014.

[6] Beliş V. Tratat de medicină legală. Ed. Medicală, Bucharest, 1995.

[7] Burch GE, Tsui CY, Harb JM. Postmortem changes in the rat myocardium. Pathobiology, 1972, 38(4):233–249.

[8] Suzuki T. An ultramicroscopic study on rigor mortis. Forensic Sci, 1976, 8(3):207–216.

[9] el-Shennawy IE, Gee DJ, Aparicio SR. Renal tubular epithelia ultrastructure in autolysis. J Pathol, 1985, 147(1):13–21.

[10] Yoshino M, Kimijima T, Miyasaka S, Sato H, Seta S. Microscopical study on estimation of time since death in skeletal remains. Forensic Sci Int, 1991, 49(2):143–158.

[11] Tomita Y, Nihira M, Ohno Y, Sato S. Ultrastructural changes during *in situ* early postmortem autolysis in kidney, pancreas, liver, heart and skeletal muscle of rats. Legal Med (Tokyo), 2004, 6(1):25–31.

[12] Şelaru M, Hostiuc S, Rusu MC. Intrinsic neuroendocrine cells in the outer wall of the human pyriform recess. Anat Sci Int, 2015, 90(4):251–255.

[13] Dermengiu D, Ceausu M, Rusu MC, Dermengiu S, Curca GC, Hostiuc S. Sudden death associated with borderline hypertrophic cardiomyopathy and multiple coronary anomalies. Case report and literature review. Rom J Leg Med, 2010, 18(1): 3–12.

[14] Rusu MC, Mănoiu VS, Vrapciu AD, Hostiuc S, Mirancea N. Altered mitochondrial anatomy of trigeminal ganglia neurons in diabetes. Anat Rec (Hoboken), 2016, 299(11):1561–1570.

[15] Penttilä A, Ahonen A. Electron microscopical and enzyme histochemical changes in the rat myocardium during prolonged autolysis. Beitr Pathol, 1976, 157(2):126–141.

[16] Karadžić R, Ilić G, Antović A, Banović LK. Autolytic ultrastructural changes in rat and human hepatocytes. Rom J Leg Med, 2010, 18(4):247–252.

[17] Badonic T, Frumkina LJ, Jakovleva NI, Hornáková A. Ultrastructural changes of neurons in dependence on the death

cause in human brain. Funct Dev Morphol, 1991, 2(4):231–234.
[18] Hukkanen V, Röyttä M. Autolytic changes of human white matter: an electron microscopic and electrophoretic study. Exp Mol Pathol, 1987, 46(1):31–39.
[19] Sheleg SV, LoBello JR, Hixon H, Coons SW, Lowry D, Nedzved MK. Stability and autolysis of cortical neurons in post-mortem adult rat brains. Int J Clin Exp Pathol, 2008, 1(3):291–299.
[20] Arsénio-Nunes M, Hossmann K, Farkas-Bargeton E. Ultrastructural and histochemical investigation of the cerebral cortex of cat during and after complete ischaemia. Acta Neuropathol, 1973, 26(4):329–344.
[21] Hibbs RG, Black WC. Electron microscopy of post-mortem changes in the rat myocardium. Anat Rec, 1963, 147(2):261–272.
[22] Muñoz DR, de Almeida M, Lopes EA, Iwamura ESM. Potential definition of the time of death from autolytic myocardial cells: a morphometric study. Forensic Sci Int, 1999, 104(2–3):81–89.
[23] Kuypers GAJ, Roomans GM. Postmortem elemental redistribution in rat studied by X-ray microanalysis and electron microscopy. Histochemistry, 1980, 69(2):145–156.
[24] Herdson PB, Kaltenbach JP, Jennings RB. Fine structural and biochemical changes in dog myocardium during autolysis. Am J Pathol, 1969, 57(3):539–557.
[25] Ludatscher RM, Hashmonai M, Peleg H. The irreversible ischaemic lesion of human myocardium. Comparison with the experimental animal model. Acta Anat (Basel), 1984, 118(2):91–95.
[26] Bassi M, Bernelli-Zazzera A. Ultrastructural cytoplasmic changes of liver cells after reversible and irreversible ischemia. Exp Mol Pathol, 1964, 3(4):332–350.
[27] Jones RT, Trump BF. Cellular and subcellular effects of ischemia on the pancreatic acinar cell. Virchows Arch B, 1975, 19(1):325–336.
[28] Ito T, Ando T, Mayahara H, Miyajima H, Ogawa K. Postmortem changes in the rat kidney. II. Histopathological, electron microscopical, and enzyme histochemical studies of postmortem changes at 0^0C. Acta Histochem Cytochem, 1991*a*, 24(2):153–166.
[29] Ito T, Ando T, Mayahara H, Miyajima H, Ogawa K. Postmortem changes in the rat kidney. I. Histopathological, electron microscopical, and enzyme histochemical studies of postmortem changes at room temperature. Acta Histochem Cytochem, 1991*b*, 24(2):135–151.
[30] McQuade HA, Evans TC. The electron microscopy of the response of follicular epithelium cells of rat thyroid to autolysis, ligation, and irradiation by Iodine-131. Radiat Res, 1959, 11(4): 520–534.
[31] Higuchi M, Abe K. Postmortem changes in ultrastructures of the mouse intervertebral disc. Spine (Phila Pa 1976), 1987, 12(1):48–52.
[32] Cingolani M, Osculati A, Tombolini A, Tagliabracci A, Ghimenton C, Ferrara SD. Morphology of sweat glands in determining time of death. Int J Legal Med, 1994, 107(3): 132–140.
[33] Carroll RJ, Cavanaugh JR, Rorer FP. Effects of frozen storage on the ultrastructure of bovine muscle. J Food Sci, 1981, 46(4):1091–1094.
[34] Hwang IH, Thompson JM. A technique to quantify the extent of postmortem degradation of meat ultrastructure. Asian Australas J Anim Sci, 2002, 15(1):111–116.
[35] Ngapo TM, Babare IH, Reynolds J, Mawson RF. Freezing rate and frozen storage effects on the ultrastructure of samples of pork. Meat Sci, 1999, 53(3):159–168.
[36] Rusu MC, Mănoiu VS, Popescu VM, Ciuluvică RC. Endothelial progenitor cells populate the stromal stem niche of tympanum. Folia Morphol (Warsz), 2017, May 29, doi: 10.5603/FM.a2017.0038.
[37] Rusu MC, Cretoiu D, Vrapciu AD, Hostiuc S, Dermengiu D, Manoiu VS, Cretoiu SM, Mirancea N. Telocytes of the human adult trigeminal ganglion. Cell Biol Toxicol, 2016, 32(3):199–207.
[38] Rusu MC, Folescu R, Mănoiu VS, Didilescu AC. Suburothelial interstitial cells. Cells Tissues Organs, 2014, 199(1):59–72.
[39] Bălăşescu E, Rusu MC, Vrapciu AD, Mirancea N, Mănoiu VS, Stan CI. Early onset of podocytes apoptosis – a TEM study in streptozotocin-induced diabetic rats. Rom J Morphol Embryol, 2014, 55(1):71–75.
[40] Rusu MC, Pop F, Mănoiu VM, Lupuşoru MO, Didilescu AC. Zipper-like series of desmosomes supported by subplasmalemmal actin belts in thymic epithelial reticular cells in the rat. Ann Anat, 2013, 195(4):359–364.
[41] Rusu MC, Didilescu AC, Stănescu R, Pop F, Mănoiu VM, Jianu AM, Vâlcu M. The mandibular ridge oral mucosa model of stromal influences on the endothelial tip cells: an immunohistochemical and TEM study. Anat Rec (Hoboken), 2013, 296(2):350–363.
[42] Rusu MC, Pop F, Hostiuc S, Curca GC, Jianu AM, Paduraru D. Telocytes form networks in normal cardiac tissues. Histol Histopathol, 2012, 27(6):807–816.
[43] Rusu MC, Mirancea N, Mănoiu VS, Vâlcu M, Nicolescu MI, Păduraru D. Skin telocytes. Ann Anat, 2012, 194(4):359–367.
[44] Madea B (ed). Estimation of the time since death. 3rd edition, CRC Press, Boca Raton, FL, USA, 2016.
[45] Burman JW. On the rate of cooling of the human body after death. Edinb Med J, 1880, 28:993–1003.

Corresponding author
Alexandra Diana Vrapciu, Lecturer, MD, PhD, Division of Anatomy, Department 1, Faculty of Dental Medicine, "Carol Davila" University of Medicine and Pharmacy, 8 Eroilor Sanitari Avenue, 050474 Bucharest, Romania; Phone +40723–303 926, e-mail: vrapciualexandra@yahoo.com

Received: January 15, 2017

Accepted: July 3, 2017